Published in final edited form as:
Int J Radiat Biol. 2009 April ; 85(4): 330–337. doi:10.1080/09553000902781139.

High dose rate radiation treatment of experimental intramuscular prostate carcinoma

Christina Skourou[1,*], **P. Jack Hoopes**[1], **Summer L. Gibbs-Strauss**[2], **David J. Gladstone**[1], **Rendall Strawbridge**[1], and **Keith D. Paulsen**[2]

[1]Dartmouth Medical School, 1 Medical Ctr. Drive, Lebanon, NH 03756, U.S.A.

[2]Thayer School of Engineering, Hanover, NH, U.S.A.

Abstract

Purpose—The Dunning R3327-MLL is a well established transplanted tumor line, and as such it makes a desirable model for evaluative studies of therapy. In the current study, the interstitial growth characteristics as well as the response of this tumor to a single fraction of high dose rate radiation is investigated.

Materials and Methods—The in-vitro response to radiation of the Dunning R3327-MLL was studied via a colony forming assay using a Cs-137 irradiator. In-vitro radiosensitivity was determined on tumors implanted intramuscularly in the left gastrocnemius muscle of the rat and irradiated using an Ir-192 afterloader.

Results—The results demonstrate a faster growth rate when compared to the reported subcutaneous growth rates. The Dunning R3327-MLL's radiosensitivity is comparable to that of late response tissues. The dose required to achieve a specific radiobiological response (the α:β ratio) of the in-vitro cell line is 2.4 Gy, whereas the ratio for the intramuscularly growing tumor was 0.99 Gy.

Conclusions—These findings signify the intramuscularly implanted Dunning R3327-MLL tumor model as a desirable model for the study of single fraction high dose rate radiation treatments.

Keywords

brachytherapy; Dunning R3327-MLL; rat; tumour radiosensitivity

Introduction

Fractionated radiation therapy (RT) is currently the standard of care for most cancer patients. The length of the treatment (up to 45 fractions) as well as the increasing volumes of normal tissue exposed by some techniques (e.g. intensity modulated RT, tomotherapy), raise the interest in methods that offer a reduction in treatment fractions as well as the amount of normal tissue exposed. To address these issues, the medical community is employing hypofractionated techniques using external beam irradiation with tight tumor margins (such is the stereotactic body radiotherapy - SBRT) as well as utilizing radioactive low-dose and high-dose sources (namely low dose rate radiotherapy – LDR - and high dose rate radiotherapy - HDR) for more conformal treatments and sparing of adjacent structures. A number of clinical trials related to these issues are currently underway, many of them investigating the effects of High Dose Rate (HDR) radiation in combination with external beam and/or chemotherapy (Sun Myint, et al., 2007). A recent protocol from the Radiation Therapy Oncology Group (RTOG 95-17),

*christina.skourou@dartmouth.edu.

investigated the use of HDR brachytherapy alone in the treatment of breast cancer after partial mastectomy. Early analyses of this study have shown that accurate dose planning and delivery is achievable with HDR brachytherapy (Ibbott, et al., 2007) which assists in maintaining normal tissue toxicity within modest and acceptable levels (Kuske, et al., 2006). Another successful application of HDR brachytherapy in the breast is the mammosite procedure which involves endocavitary irradiation with the aid of a balloon positioned in the breast following partial mastectomy (Benitez, et al., 2007). Similar successes have been reported for rectal (Vuong, et al., 2007), cervical (Kazumoto, et al., 2007), and prostate (Kälkner, et al., 2007) cancer HDR brachytherapies. Despite the high level of clinical interest being expressed over HDR treatment, very few animal studies are being conducted to provide formative histopathological and radiobiological information. One important reason for the lack of animal studies is the limited options for selecting an appropriate animal model.

The choice of biological model for studying injury and disease underpins the clinical relevance and applicability of the observed results. Biological models range in complexity from in vitro cell cultures to mammalian in vivo systems. As models advance in complexity, the choice of organism as well as the design of the experiment becomes increasingly important and extrapolation of the results into clinical practice becomes more convoluted. In the case of small animal models, differences in lifetime, organ/tissue size, and metabolism should be taken into consideration when clinical conjectures are offered. In the study of interstitial high dose rate irradiation in animals, questions of tumor versus surrounding normal tissue volume and accurate tumor localization within that tissue need to be addressed.

Formation of malignant tumors evolves through progressive transitions from benign hyperproliferative lesions containing atypia (cellular and architectural) to locally expanding masses with metastatic propensity. In an experimental setup, this process can be mimicked through the use of carcinogens, or by exposure of the animals to highly toxic environments. Although the process can be very controlled and repeatable, the resulting tumors will almost certainly differ in location and onset time (spontaneous tumorigenesis). In HDR brachytherapy studies, repeatability in terms of location and growth rate is significant; thus, the most reliable method for tumor induction occurs via tissue implant or cell suspension inoculation. The major drawback in these methods is the alteration of the microenvironment in which the tumor develops. Human derived tumor cell lines are often used as xenografts in rodent experiments aiming to explain tumor response to therapy. With the exception of orthotopic tumor inoculation (e.g. prostate), most tumor cells are implanted subcutaneously. This location facilitates accessibility to the tumor whether for size measurements or direct administration of drugs or other treatments. In radiation studies, the response of the host system is also of interest and therefore subcutaneous tumor growth is not as desirable; instead, intramuscular growth is preferred.

Given the clinical interest in HDR radiotherapy, yet the modest amount of in vivo preclinical work that has appeared on the technique in part because of the importance of having a well-understood interstitially implanted tumor cell line (rather than the usual subcutaneous model system which has dominated the landscape of small animal cancer studies) to evaluate the therapy appropriately, the aim of this paper is twofold. First, the Dunning R-3327-MLL tumor (MLL) is a model system whose in vitro and subcutaneous in vivo behavior has been adequately described in the literature (Smolev, et al., 1977, Isaacs, et al., 1978, Isaacs, et al., 1981, Lohr, et al., 1993) but whose interstitially implanted characteristics have not been reported. Here, we contribute to the characterization of this important tumor cell line by describing its behavior in an intramuscular environment in terms of site migration after implantation, uptake fraction and growth rate reproducibility. Second, the response of the intramuscularly implanted Dunning R-3327-MLL tumor to HDR brachytherapy is presented to evaluate the success of a single HDR fraction delivered interstitially in eradicating a tumor while maintaining normal

tissue integrity. The radiosensitivity of the MLL tumor line to a single fraction of HDR treatment is also investigated.

Methodology

The Dunning R3327-MLL tumor

The Dunning R3327-MLL tumor cell line is derived from the Dunning R3327-H tumor through a series of in vitro passages and share many of its growth kinetic characteristics (Isaacs, et al., 1981). It produces a fast growing, androgen insensitive, anaplastic tumor which is highly metastatic to lymph nodes and lungs (Kal, et al., 2004) and has been reported to possess a morphology and a physiology that is similar to human prostate cancer (Smolev, et al., 1977, Isaacs, et al., 1978). Lohr et al. report that the R3327-H tumor has an S-phase duration T_s of 8 hours, a labeling index ($L.I.=\lambda \times \frac{T_s}{T_c}$, where λ is the percentage of cells proliferating and T_c is the total generation time) of 7±0.5% (measured with flow cytometry), a potential cellular doubling time (T_{pot}) of 4.7 days and a cell loss factor $(\varphi=1-\frac{T_{pot}}{T_D})$ where T_D is the clinically observed volume doubling time) of 15% (Lohr, et al., 1993).

More recently, the MLL has been lending itself to orthotopic studies regarding the efficacy of treatments for prostate cancer. Examples include nanoparticle therapy (Johannsen et al, 2006), photodynamic therapy (Zhoo et al, 2006), chemotherapy (Shikanov et al, 2008) and diagnostic applications for differentiation of malignant and normal tissues (Gemeinhardt et al, 2005). Zechmann et al (2007) have compared the morphological characteristics of subcutaneous and orthotopic Dunning R-3327 tumors. Interestingly, they have found that the rate of growth, even though it is significantly different between orthotopically and subcutaneously growing tumors, depends on cell line more than location. The Dunning R-3327-AT1 and Dunning R-3327-H cell lines grew faster when implanted subcutaneously, while the Dunning R-3327-H1 grew faster when implanted orthotopically.

We have previously studied the growth pattern of the MLL when implanted intramuscularly (Skourou, et al., 2007). From our experience, the MLL line has an in vitro doubling time of 8 to 10 hours with an observed in vivo initial volume doubling time of 1.11 days. The in vivo doubling time is faster than the approximately 3 days reported by Kal et al. (Kal, et al., 2004), Isaacs et al. (Isaacs, et al., 1981), Harms et al. (Harms, et al., 2002), and Tennant et al. (Tennant, et al., 2000). The doubling times that are described by these authors are for tumors growing subcutaneously in the flank of the animal, whereas our tumors were implanted intramuscularly in the leg. A comparative plot showing the difference between the tumor volume increase for the RIF-1 tumor (a murine radiation induced fibrosarcoma) grown subcutaneously versus tumors grown intramuscularly in the leg can be found in Kallman's book (Kallmann R, 1987) which states that the volume doubling time for intramuscularly grown tumors is almost twice as fast as that of subcutaneous tumors. The intramuscular acceleration is attributed to the ample blood supply pre-existing in the muscle (relative to the lack of it in subcutaneous areas) and corroborates our observed doubling times. By comparison, an orthotopically growing MLL tumor grows even faster – ten days post implant, an orthotopically growing MLL tumor is reported to have a volume of 0.74 cm^3 (Johannsen et al., 2006) whereas an intramuscularly growing one is 0.57 cm^3 (Skourou et al., 2007).

The Dunning R-3327 is an established transplanted tumor line, and as such makes a desirable model for evaluative studies of therapy. Assays exist for determining tumor growth delay, clonogenic cell survival, and cure. Through this model, the mechanisms of action of different treatment modalities have been investigated and the role of factors such as cell-cycle

redistribution, repopulation, reoxygenation, hyperthermia, repair and drug uptake in the overall tumor response have been assessed (Thorndyke, et al., 1985, Lohr, et al., 1993, Rao, et al., 1991, Peschke et al., 1998, Harms, et al., 2002, Kal, et al., 2004, Chen, et al., 2006, Bourke et al., 2007).

A concern that rises with MLL use is its rapid proliferation. In terms of experimentation, this characteristic is of great value since it results in high plating efficiency and, from our experience, in 100% uptake fraction. However, it limits use of fractionation during radiation studies since its lifetime does not allow enough time between fractions (typically 1 week). In addition, the vasculature is unable to maintain growth at the same pace which results in nutrient deficient subpopulations of cells in a manner not consistent with slower growing human cancers. With these characteristics taken into consideration, the response of the Dunning R3327-MLL is studied after a single fraction of high dose rate radiation delivered directly to the center of the tumor at an early stage (5 days post implantation) prior to the development of central necrosis in the tumor.

In vitro cell survival assessment

All Dunning R3327-MLL cells were maintained at 37 degrees Celsius, 5% CO_2. Cells were grown to near confluence in T25 flasks in alpha Minimum Essential Medium (MEM) media supplemented with 10% fetal calf serum (Sigma-Aldrich, St-Louis, MO, USA). Four hours prior to treatment, the cells were harvested, counted and serially diluted to make final concentrations of 100 and 200 cells per well in a 6-well plate. All samples were plated in triplicate. Cells were treated with one of the experimental groups (0 Gy, 2 Gy, 4 Gy, 6 Gy, and 8 Gy). Irradiation has been performed in house on a Cs-137 irradiator. Following treatment 6-well plates were incubated (37 degrees, 5% CO_2) for approximately 7 days. On the 7^{th} day, the media was aspirated from the dish, and approximately 3 ml of 1% methylene blue (Sigma-Aldrich) in 10% methanol was added to fix and stain the colonies. The cells were incubated at room temperature for 1 minute. The stain/fixative was poured off and the plate was flushed with water. Once air dry, the colonies were counted under a microscope.

Implantation accuracy

Since localization of an intramuscular (IM) tumor to be treated with interstitial HDR is of crucial importance, a substudy was designed to detect the growth location of tumors. Twelve animals were implanted with 10^5 MLL cells intramuscularly ($t = t_0$). An anatomic positioning device was used to ensure the repeatable insertion of the cell inoculation needle, as well as the insertion of the brachytherapy delivery catheter, laterally on the leg (Skourou, et al., 2004). Five days later ($t = t_5$), the animal was perfused with 4% neutral-buffered formaldehyde while under deep anesthesia. A heparin injection (2 ml/kg) minimized vascular blood clotting. The abdominal cavity of the animal was surgically exposed and a 24 GA-19 mm catheter was inserted in the descending aorta approximately 1 cm proximal to the femoral artery bifurcation. The vena cava was tied off at the same location and a longitudinal arteriotomy was performed to allow for the return flow to exit the system. If necessary, the animal was euthanized with an intracardiac injection of saturated potassium chloride (KCl) post perfusion. The legs were detached from the body at the femur head. The skin was removed and the leg was immersed overnight in 10% formaldehyde solution. The following day, 3 tissue slices were collected from the treated leg and were processed using standard pathology protocols to yield microscopic slides for histological evaluation. An initial slice of tissue was collected along the plane of implantation (section A); two additional slices were obtained 3mm superior and inferior to that plane (sections B and C).

High Dose Rate radiation delivery

Thirty six animals were implanted with 10^5 MLL cells ($t = t_0$) and randomized in three dose groups: 26 Gy, 39 Gy, and 52 Gy delivered in a single fraction of high dose rate (HDR) radiation. The algorithm used for the dose calculation (BrachyVision™, Varian Medical Systems, Inc., Pao Alto, CA, USA) is based on the AAPM TG43 protocol which accounts for the variation of relative dose due to spatial distribution of activity within the source (geometry factor), for the effects of absorption and scatter in the medium along the transverse axis of the source (radial dose factor), and for the anisotropy of the dose distribution around the source (anisotropy factor) (Rivard, et al., 2004). Radiation was delivered interstitially five days following tumor cell inoculation ($t = t_5$). On the day of treatment, the animals were transferred to the Radiation Oncology department of the Norris Cotton Cancer Center, Lebanon, NH, USA where they were anesthetized with 4% isoflurane gas. A Varian Varisource 200® afterloader (Varian Medical Systems, Inc.) with an Iridium-192 source was employed to deliver the prescribed dose. A 21 GA (1.2 mm) - 10 cm long interstitial needle was inserted in both legs with the aid of the anatomical positioning device. The needle from the tumor bearing leg was then connected to the afterloader via an 80 cm long coupling catheter. The afterloader temporarily inoculated the radioactive seed in the catheter which stayed in place long enough to deliver the desired dose of radiation. Upon completion of treatment, the needles from both legs were removed, and the animal was allowed to recover from anesthesia before being returned to the animal housing facility. The animals were followed via palpation twice a week. The end-points of this study were determined when a clearly palpable mass was present in the leg, or 10 weeks had passed after tumor irradiation, which ever event occurred first.

All animal activities were approved by the Dartmouth College Institutional Animal Care and Use Committee and follow all United States Department of Agriculture (USDA) and Association for Assessment and Accreditation of Laboratory Animal Care International (AAALAC) guidelines.

Results and Discussion

In vitro characterization of the radiosensitivity of the Dunning R3327-MLL tumor

In Skourou et al. (Skourou, et al., 2007), the behavior of a primary rat tumor resulting from the implantation of viable tumor cells was presented. The growing tumor volumes, as calculated from Magnetic Resonance (MRI) images, were fitted to an exponential curve ($V(t) = V_0 e^{\lambda t}$) with $\lambda = 0.622$ and a predicted volume doubling time of 1.11 days. Prior to investigating the radiosensitivity of the intramuscularly growing tumor, the in vitro response is described.

The results from the colony-forming assay are shown in Figure 1. The linear-quadratic model was used to describe this survival curve. The model assumes that there are two components to cell killing by radiation, a linear one (α), and one of which (β) is proportional to the square of the dose (D) (Hall, et al., 2000). The expression for the cell survival curve based on this model is:

$$S = e^{-\alpha D - \beta D^2}$$

The α:β ratio as determined from the model was 2.424 Gy. This is the dose at which the killing from linear and quadratic components is equal. Also from this model we can extract D_1, the dose required to reduce the fraction of surviving cells to 37%, equal to 4.1 Gy; it is mathematically the slope of the initial part of the curve. D_0 is another important parameter, which is the dose needed to reduce the fraction of surviving cells to 37% of its current level, equal to 0.97 Gy; it is the slope of the final part of the curve. Hall suggests using yet another parameter when describing the survival characteristics of cells, D_{10} (Hall, et al., 2000). This

parameter reflects the dose required to reduce the number of cells by one decade. For example, in a tumor containing 10^5 cells with a D_0=0.97 Gy, a dose of 11.2 Gy will eliminate all 10^5 cells ($5 \times D_{10} = 5 \times \ln(10) \times D_0 = 11.2$ Gy).

In order to estimate the number of cells per unit volume in the MLL tumor 5 days post implantation ($t = t_5$), the number of cells included in a 0.1×0.1 mm^2 area was counted on a morphological slide and was found to be 58. Assuming a uniform and symmetrical distribution of cells, a volume of 1 mm^3 contains 3364×10^3 cells. Five days post intramuscular implantation of the MLL cells, according to Skourou et al. (Skourou, et al., 2007), the MLL tumor has an average volume of 0.04 cc (40 mm^3), i.e. 1.3×10^8 cells. Using the previous formula, a dose of $9\times \ln(10) \times D_0 = 20$ Gy should suffice to eradicate all tumor cells. However, tumor response to radiation changes significantly in vivo mainly due to environmental factors (availability of blood supply, oxygenation, inflammatory response, intercellular signaling, etc.). It is therefore reasonable to expect that the D_{10} threshold will increase significantly under in vivo conditions.

Tumor size variability—All animals implanted with MLL tumor cells for the purposes of this study have developed a palpable mass by the 5th day following implantation. The MLL tumor contains approximately 3364×10^3 cells and has a volume of 0.04 cc five days after inoculation of 10^5 MLL cells intramuscularly. This tumor size is ideal because it can be included within a radiation field of 5 mm radius around the high dose rate Ir-192 radioactive seed. This field spares the skin from damaging exposure allowing the administration of relatively large doses in the tumor area in a single fraction (Figure 2). However, identical and ideal conditions are very difficult to achieve in vivo, in which case quantification of the variability is necessary. Twelve animals were inoculated with 10^5 MLL cells and were subsequently sacrificed 5 days post implantation. The tumor location and size were then determined on histological samples.

Typically, a solid tumor was found growing at the edge of the muscle fascicle between the gastrocnemius and the extensor digitorum muscles. Table I shows the diameters of the tumors in the 12 animals, as well as their location. Note that in four of the twelve animals no solid tumor was detected. Signs of malignancy (such as extensive inflammatory edema) were always evident in at least one of the histological sections.

The results included in Table I show that there is ±0.98 mm variability (2 × standard error) in diameter (for 95% confidence interval) around the mean. This implies that 95% of all tumors at $t = t_5$, will have diameters between 1.04 mm and 3.00 mm. The table also indicates that 75% of the implanted tumors grow within 3 mm from the location of initial cell inoculation, with 50% of them growing in the same plane. A diameter of 4.0 mm was used in the statistical analysis wherever the tumor was visible in more than one plane.

Brachytherapy—Benefits of using HDR radiation for treatment include the tight isodose curves around the seed and the rapid drop in dose with distance from the source which makes the administration of high doses in single fractions possible without much complication to tissues relatively close to the target volume (Figure 2). In the case of the animal leg, the most sensitive structure in the field is the skin. However, even at the 52 Gy dose, the exposure to the skin is around 30 Gy which is well tolerated.

Radiation injury to muscle and tumor—The volume effect, i.e. the dependence of the radiation damage to normal tissues on the volume of tissue irradiated (Hall, et al., 2000) is one of the issues that complicated our animal model. The disproportionality of the amount of malignant tissue relative to the surrounding normal tissue (muscle and skin) poses a challenge to delivering a treatment that closely resembles a clinical exposure. Our previous studies with

this animal/tumor model (Skourou, et al., 2007) have shown that the amount of malignant tissue reaches up to 50% of the amount of the normal tissue in the treatment field, a ratio that rarely occurs in the treatment of human cancers. However, at the time chosen for irradiation ($t = t_5$) the situation is more representative of a clinical case where the tumor volume is 5% of the surrounding normal tissue. Using muscle as the host organ also decreases the volume effect because its functional subunits (fascicles) are arranged in parallel (as opposed to serially like the spinal cord). Thus, if a vessel or a fiber is damaged, the surrounding fibers continue to function, and healing occurs from surviving clonogens scattered throughout the treatment volume (Hall, et al., 2000). Persons et al studied the effects of radiation on rat skeletal muscle by following animals irradiated at single fraction doses of 15 Gy, 30 Gy, 45 Gy and 60 Gy. They show that for an adult rat, in the first 10 weeks following radiation, the muscular volume of the lower leg (calf) is reduced by 17.5%, and its wet weight dropped by 28% (Persons, et al., 2001). Interestingly, their results indicate a large difference in the response depending on the age of the animal, but show no difference with increasing dose. This can be explained by the difference in the percent incidence of satellite cells between young and adult rats. A year later, the muscular volume did not undergo any further reduction, whilst the wet weight continued to decrease as scarring replaced the injured tissue. In our experiments the maximum dose received by 50% of the tissue does not exceed 44 Gy. Our follow-up period is 10 weeks, during which time we expect to see some reduction in muscle volume and normal fiber count in the irradiated tissue, but this effect is expected to be comparable at all doses (26 Gy, 39 Gy, and 52 Gy).

The effect of interweaving of tumor with normal tissues is reduced through the use of interstitial HDR brachytherapy. The intramuscular transplantation of MLL tumor cells induces an acute immune response which results in edema concentrated at the muscle/tumor boundary. Peritumoral edema is also found accompanying human soft tissue sarcomas as well as most pediatric brain tumors (Bartkowski, et al, 1984). Its presence poses a challenge for radiation therapy planning and delivery. Interstitial HDR treatment ensures that maximum doses are indeed delivered within the tumor mass and, in our case, the 5 mm isodose prescription encompasses the whole tumor while providing a large enough margin to ensure sufficient irradiation of the tissues past the edge of the edematous zone where active malignant cells are also typically found.

Calcification and pseudocapsule formation were never observed in the studies completed here. Since the animals were sacrificed at the end of the 10-week period, no conclusion can be made with certainty as to whether differentiation is a complication in our model. Fibrosis in the form of interstitial thickening was a prominent late effect at all doses. Edema, muscular degeneration, and necrosis were also observed soon after radiation and were more pronounced at the higher doses.

In vivo characterization of the radiosensitivity of the R3327-MLL tumor—Table II shows the recurrence pattern for the implanted tumors after receiving radiation doses of 26 Gy or 39 Gy or 52 Gy. As suspected from the in vitro studies, 26 Gy achieved no local tumor control. With 39 Gy, 42 % of the animals responded well, while tumor recurrence (defined as the time of the first sign of tumor presence via palpation) was observed as early as 6 weeks post irradiation for the other 50 %. The highest dose successfully eradicated the tumor; however, extensive muscle degeneration and interstitial thickening were observed at the time of sacrifice near the 100 % isodose plane. The dose at the skin did not exceed 30 Gy. The only indication visible was a slight erethyma on the leg 2–3 days post treatment which subsided by the end of the first week. The animals from all dose groups maintained normal use of their hind legs at all times.

The data at the end of the observation period (10 weeks post treatment) were used as the endpoint to determine the radiosensitivity of the intramuscular tumor to HDR. The linear-quadratic model was used as described earlier to yield an in-vivo α:β ratio close to unity and D_{10} = 68.67 Gy. This D_{10} value is three times higher than the one predicted from the in vitro study. With the 100% isodose line (52 Gy) of the high dose group prescribed at 5 mm from the implantation point, a large percentage of the tumor has received 64.5 to 78 Gy (125–150%). The successful eradication of tumors in this group confirms the predicted D_{10} value.

Conclusion

Transplantation site, uptake fraction, reproducible growth behavior, and response to treatment are all factors of potential importance when selecting a tumor model for preclinical studies (Siemann, 1987). The Dunning R-3327-MLL tumor has been previously used in therapeutic investigations. Its in vitro, as well as its in vivo subcutaneous behavior have been adequately described in literature as was referenced throughout the manuscript. The present work adds to the characterization of this tumor cell-line by describing its behavior in an intramuscular environment. We have shown that there is minimal cell migration from the implantation point to the tumor growth location (2–4 mm), with a preference evident for interfascial locations. A satisfactory tumor uptake has been demonstrated, and a growth repeatability of approximately 1 mm in tumor diameter at 5 days after cell inoculation was found. The tumor response to a single fraction of high dose rate radiation administered to the center of the tumor has also been investigated. The in vitro predicted dose of 20 Gy was inadequate for tumor eradication in the in vivo setting. A tumor growth delay of up to 5 weeks was observed after administration of 26 Gy as a single fraction HDR brachytherapy. A dose of 39 Gy single fraction achieved 50 % cure with a 42 % recurrence observed at 6–8 weeks post treatment. The high dose of 52 Gy single fraction was successful in total tumor eradication, with noted fibrosis of the muscle at the 100 % isodose line. Application of the linear-quadratic model on both the in vitro and the in vivo data has shown a change of 1.4 in the α:β ratio and a threefold increase of the D_{10} value.

The HDR form of radiation delivery exposes the tumor site to very high doses while sparing the surrounding normal tissue structures. Clinical interest in HDR has increased in recent years. The detailed characterization of the MLL tumor model and its response to this form of therapy make it an effective and valuable model for the study of cancerous and normal tissue response following HDR treatment in an experimental preclinical setting.

References

Benitez P, Keisch ME, Vicini F, Stolier A, Scroggins T, Walker A, et al. Five-year results: the initial clinical trial of MammoSite balloon brachytherapy for partial breast irradiation in early-stage breast cancer. American Journal of Surgery 2007;194:456–462. [PubMed: 17826055]

Chen B, Pogue B, Luna J, Hardman R, Hoopes PJ, Hasan T. Tumor vascular permeabilization by vascular-targeting photosynthesization: effects, mechanism, and therapeutic implications. Clinical Cancer Research 2006;12:917–923. [PubMed: 16467106]

Bartkowski HM. Peritumoral edema. Progress in Experimental Tumor Research 1984;27:179–190.

Bourke VA, Zhao D, Gilio J, Chang CH, Jiang L, Hahn EW, Mason RP. Correlation of Radiation Response with Tumor Oxygenation in the Dunning Prostate R3327-AT1 Tumor. International Journal of Radiation Oncology, Biology, Physics 2007;67:1179–1186.

Gemeinhardt O, Lüdemann L, Prochnow D, Abramjuk C, Taupitz M, Hamm B, Beyersdorff D. Differentiation of prostate cancer from normal prostate tissue in an animal model: conventional MRI and dynamic contrast-enhanced MRI. Fortschritte auf dem Gebiete der Röntgenstrahlen und der Nuklearmedizin 2005;177:935–939.

Hall, EJ.; Giaccia, AJ. Philadelphia: Lippincott Williams & Wilkins; 2000. Radiobiology for the radiologist.

Harms W, Peschke P, Weber K, Hensley F, Wolber G, Debus J, et al. Dose-dependent differential effects of low and pulsed dose-rate brachytherapy in a radioresistant syngenic rat prostate tumour model. International Journal of Radiation Biology 2002;78:617–623. [PubMed: 12079541]

Ibbott GS, Hanson WF, O'Meara E, Kuske RR, Arthur D, Rabinovitch R, et al. Dose specification and quality assurance of radiation therapy oncology group protocol 95-17; a cooperative group study of iridium-192 breast implants as a sole therapy. International Journal of Radiation Oncology, Biology, Physics 2007;69:1572–1578.

Isaacs JT, Heston WD, Weissman RM, Coffey DS. Animal Models of the Hormone-sensitive and -insensitive Prostatic Adenocarcinomas, Dunning R-3327-H, R-3327-HI, and R-3327-AT. Cancer Research 1978;38:4353–4359. [PubMed: 698976]

Isaacs J, Yu G, Coffey D. The characterization of a newly identified, highly metastatic variety of the Dunning R 3327 rat prostatic adenocarcinoma system: The MatLyLu tumor. Investigative Urology 1981;19:20–24. [PubMed: 7251319]

Johannsen M, Thiesen B, Gneveckow U, Taymoorian K, Waldöfner N, Scholz R, Deger S, Jung K, Loening SA, Jordan A. Thermotherapy using magnetic nanoparticles combined with external radiation in an orthotopic rat model of prostate cancer. Prostate 2006;66:97–104. [PubMed: 16114060]

Kal H, Struikmans H, Gebbink M, Voest E. Response of rat prostate and lung tumors to ionizing radiation combined with the angiogenesis inhibitor AMCA. Strahlentherapie und Onkologie 2004;180:798–804. [PubMed: 15592700]

Kälkner KM, Wahlgren T, Ryberg M, Cohn-Cedermark G, Castellanos E, Zimmerman R, et al. Clinical outcome in patients with prostate cancer treated with external beam radiotherapy and high dose-rate iridium 192 brachytherapy boost: a 6-year follow-up. Acta Oncologica 2007;46:909–917. [PubMed: 17917823]

Kallmann, R. New York: Pergamon Press; 1987. Rodent tumor models in experimental cancer therapy.

Kazumoto T, Kato S, Tabushi K, Kutsutani-Nakamura Y, Mizuno H, Takahashi M, et al. High dose-rate intracavitary brachytherapy for cervical carcinomas with lower vaginal infiltration. International Journal of Radiation Oncology, Biology, Physics 2007;69:1157–1166.

Kuske RR, Winter K, Arthur DW, Bolton J, Rabinovitch R, White J, et al. Phase II trial of brachytherapy alone after lumpectomy for select breast cancer: toxicity analysis of RTOG 95-17. International Journal of Radiation Oncology, Biology, Physics 2006;65:45–51.

Lohr F, Wentz F, Flentje M, Peschke P, Hahn E. Measurements of the proliferative activity of three different sublines of the Dunning rat prostate tumor R3327. Strahlentherapie und Onkologie 1993;169:438–445. [PubMed: 8342118]

Persons C, Hermens A, Franken N, Wondergem J. Muscle wasting after radiotherapy in young and adult rats. Oncology Reports 2001;8:1117–1121. [PubMed: 11496327]

Peschke P, Hahn EW, Wenz F, Lohr F, Braunschweig F, Wolber G, Zuna I, Wannenmacher M. Differential sensitivity of three sublines of the rat Dunning prostate tumor system R3327 to radiation and/or local tumor hyperthermia. Radiation Research 1998;150:423–430. [PubMed: 9768856]

Rao B, Slotman B, Geldof A, Perez C. Radiation sensitivity of Copenhagen rat prostatic carcinoma (R3327-AT and R3327-MATLyLu). International Journal of Radiation Oncology, Biology, Physics 1991:981–985.

Rivard MJ, Coursey BM, DeWerd LA, Hanson WF, Huq MS, Ibbott GS, Mitch MG, Nath R, Williamson JF. Update of AAPM Task Group No. 43 Report: A revised AAPM protocol for brachytherapy dose calculations. Medical Physics 2004;31:633–674. [PubMed: 15070264]

Shikanov S, Shikanov A, Gofrit O, Nyska A, Corn B, Domb AJ. Intratumoral delivery of paclitaxel for treatment of orthotopic prostate cancer. Journal of Pharmaceutical Sciences. 2008 [Epub].

Siemann, D. Satisfactory and unsatisfactory tumor models: factors influencing the selection of a tumor model for experimental evaluation. In: Kallmann, R., editor. Rodent tumor models in experimental cancer therapy. New York: Pergamon Press; 1987. p. 12-15.

Skourou C, Hoopes PJ, Strawbridge R, Paulsen KD. Feasibility studies of electrical impedance spectroscopy for early tumor detection in rats. Physiological Measurement 2004;25:335–346. [PubMed: 15005327]

Skourou C, Rohr A, Hoopes PJ, Paulsen KD. In vivo EIS characterization of tumour tissue properties is dominated by excess extracellular fluid. Physics in Medicine and Biology 2007;52:347–363. [PubMed: 17202619]

Smolev JK, Heston WD, Scott WW, Coffey DS. Characterization of the Dunning R3327H prostatic adenocarcinoma: an appropriate animal model for prostatic cancer. Cancer Treatment Reports 1977;61:273–287. [PubMed: 872132]

Sun Myint A, Lee CD, Snee AJ, Perkins K, Jelley FE, Wong H. High dose rate brachytherapy as a boost after preoperative chemoradiotherapy for more advanced rectal tumors: the Clatterbridge experience. Clinical oncology (Royal College of Radiologists) 2007;19:711–719.

Tennant T, Kim H, Sokoloff M, Rinker-Schaeffer C. The Dunning model. The Prostate 2000;43:295–302. [PubMed: 10861749]

Thorndyke C, Meeker B, Thomas G, Lakey W, McPhee M, Chapman J. The radiation sensitivities of R3327-H and R3327-AT rat prostate adenocarcinomas. Journal of Urology 1985;134:191–198. [PubMed: 4009821]

Vuong T, Devic S, Podgorsak E. High dose rate endorectal brachytherapy as a neoadjuvant treatment for patients with resectable cancer. Clinical Oncology 2007;19:701–705. [PubMed: 17714925]

Zechmann CM, Woenne EC, Brix G, Radzwill N, Ilg M, Bachert P, Peschke P, Kirsch S, Kauczor HU, Delorme S, Semmler W, Kiessling F. Impact of stroma on the growth, microcirculation, and metabolism of experimental prostate tumors. Neoplasia 2007;9:57–67. [PubMed: 17325744]

Zhou X, Chen B, Hoopes PJ, Hasan T, Pogue BW. Tumor vascular area correlates with photosensitizer uptake: analysis of verteporfin microvascular delivery in the Dunning rat prostate tumor. Photochemistry and Photobiology 2006;82:1348–1357. [PubMed: 17421078]

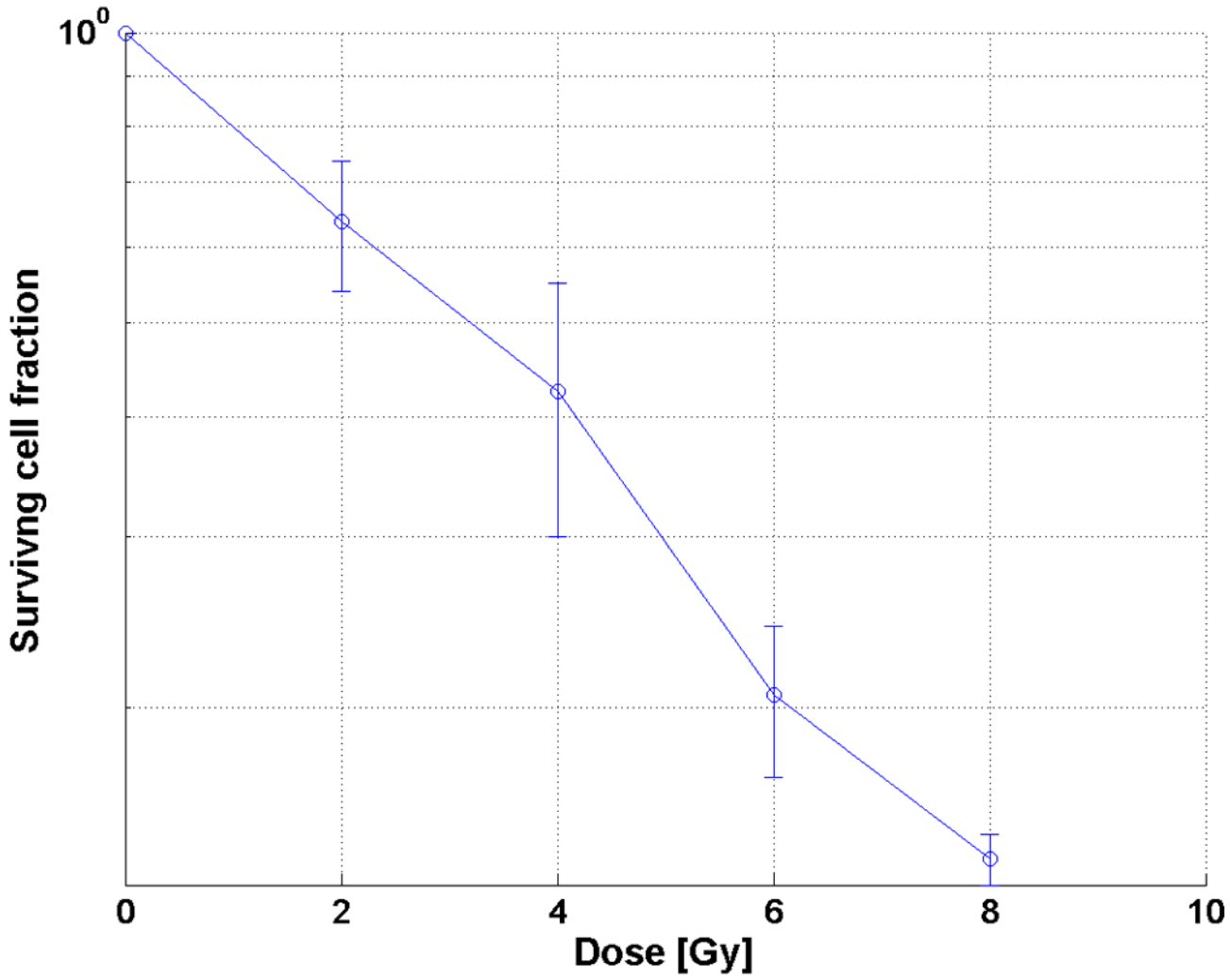

Figure 1.

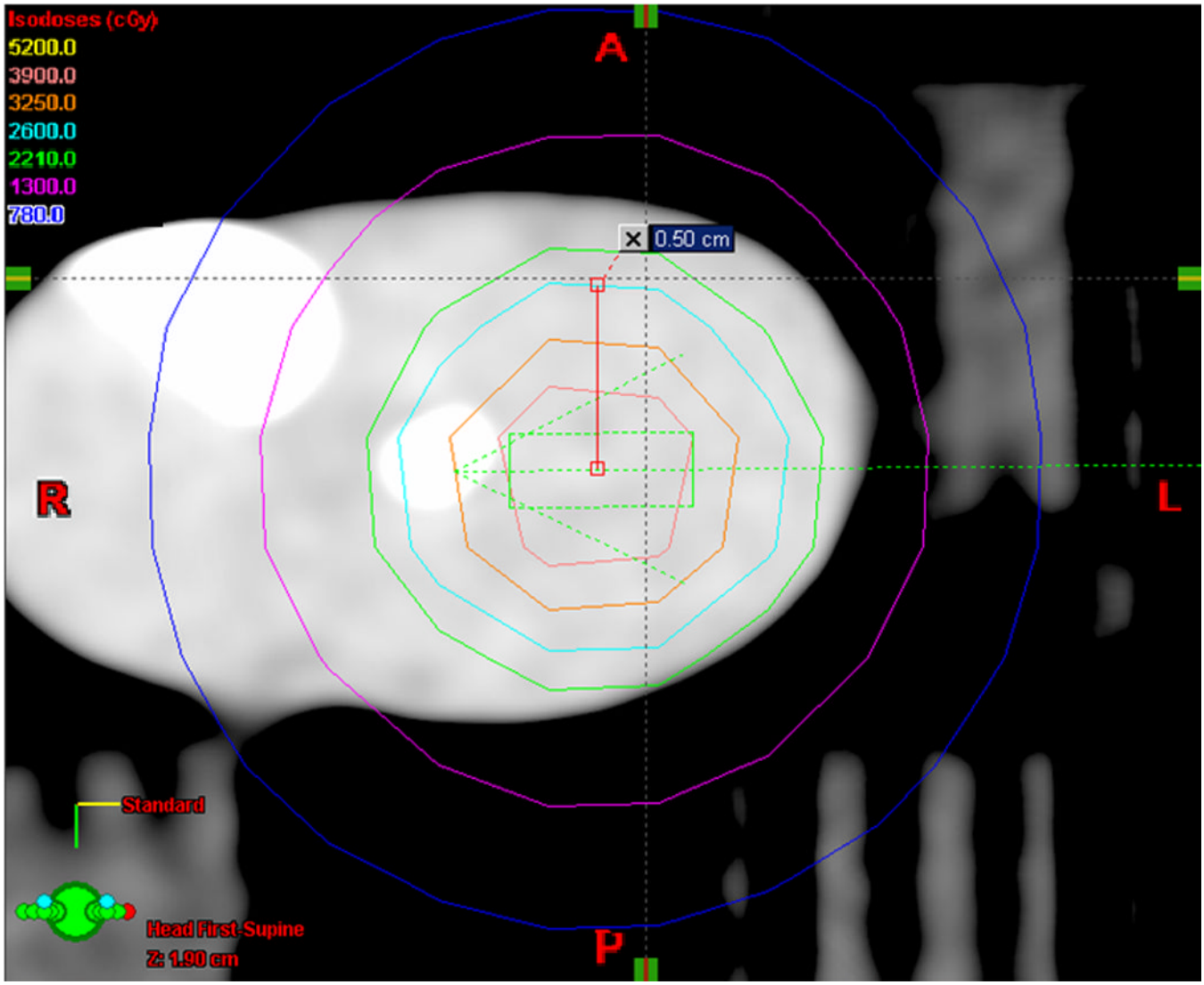

Figure 2.

Table I

Diameters and locations of non-irradiated tumors at $t = t_5$ (N=12).

Animal Number	Location (A/B/C)	Measured Diameter [mm]
269217	A/B	0.8/2.7
269218	-	-
269219	-	-
269220	B	1.9
269221	C	4.0
269225	B	2.6
269226	-	-
269227	B/C	1.1/2.5
269228	-	-
269229	B	2.5
269230	C	1.3
269231	B/C	2.1/3.1
Mean		**2.02**
Standard Deviation		**1.73**

A: section along the implantation plane. B, C: sections 3 mm superior and inferior to the implantation plane, respectively.

Table II

Recurring tumor timeline after 26 Gy, 39 Gy, and 52 Gy HDR irradiation. Recurrence was determined by palpation or histology. N=12 per dose group.

Dose	Weeks post tumor irradiation									
	1	**2**	**3**	**4**	**5**	**6**	**7**	**8**	**9**	**10**
26 Gy	1/12	3/12	2/12	3/12	3/12	-	-	-	-	-
39 Gy	0/12	0/12	0/12	0/12	0/12	1/12	1/12	3/12	0/12	0/12
52 Gy	0/12	0/12	0/12	0/12	0/12	0/12	0/12	0/12	0/12	0/12

Int J Radiat Biol. Author manuscript; available in PMC 2010 April 1.